## **Infra-Red Activities of Adsorbed Species on Metal Surfaces:**

## The Puzzle of Adsorbed Methyl (CH<sub>3</sub>)

Xueyao Zhou,<sup>1</sup> Harmina Vejayan<sup>2</sup>, Rainer D. Beck,<sup>2</sup>, Hua Guo,<sup>3</sup> and Bin Jiang<sup>1,\*</sup>

<sup>1</sup>Hefei National Laboratory for Physical Science at the Microscale, Department of Chemical Physics, University of Science and Technology of China, Hefei, Anhui

230026, China

<sup>2</sup>Institute of Chemical Sciences and Chemical Engineering (ISIC), École

Polytechnique Fédérale de Lausanne (EPFL), 1015 Lausanne, Switzerland

<sup>3</sup>Department of Chemistry and Chemical Biology, University of New Mexico,

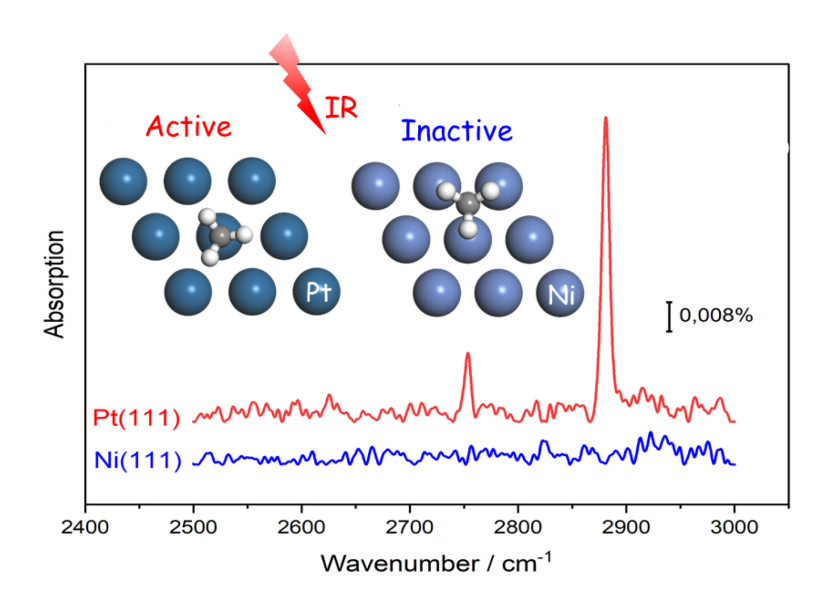
Albuquerque, New Mexico 87131, USA

<sup>\*:</sup> corresponding author, email: bjiangch@ustc.edu.cn.

## **Abstract**

Reflection absorption infra-red spectroscopy (RAIRS) is widely used to identify molecular adsorbates on metals during surface chemical reactions, but the interpretation of RAIRS data is often difficult with experiment alone. Here, we reveal from first-principles the origin of the contrasting RAIRS spectra of methyl adsorbed on Pt(111) and Ni(111). We find that the dynamic dipole along surface normal associated with the symmetric C-H stretch vibration of CH<sub>3</sub> is significant on Pt(111) but negligibly small on Ni(111), explaining the strong IR activity in the former while the absence of any RAIRS peaks in the latter. This difference is correlated with different charge transfer patterns between metals and the adsorbate, which turn out to be determined by the different preferred adsorption sites of methyl on the two surfaces. This work highlights the need of electronic structure calculations in interpreting RAIRS spectra of adsorbates on metal surfaces.





Reflection absorption infra-red spectroscopy or infra-red absorption spectroscopy (RAIRS or IRAS) is a powerful and widely used technique for high-resolution vibrational spectroscopy of adsorbates on solid surfaces using a Fourier transform infrared spectrometer.<sup>1-2</sup> For adsorbed species on metallic surfaces, the so-called surface selection rule states that RAIRS detects only vibrational transitions associated with a change in dipole moment perpendicular to the surface. RAIRS detection was first applied to study the vibrations of chemisorbed CO on different surface sites,<sup>1</sup> leveraging the large dynamic dipole and surface site specific frequency shifts of the adsorbed CO.<sup>3-4</sup> Analysis of the frequency shifts and application of the surface selection rule helped to reveal the relationship between the coordination number of surface atoms and the adsorbate.

More recently, RAIRS has been used to investigate chemisorption reactions on catalytically relevant metal surfaces,<sup>5</sup> especially in state- and site-resolved experiments.<sup>6-8</sup> Compared with other surface sensitive detection techniques such as temperature programmed desorption (TPD) and Auger electron spectroscopy (AES), RAIRS has the advantage of being a non-invasive technique allowing for *in-situ* detection of reaction products and intermediates.<sup>9</sup> For example, the dissociative chemisorption of methane on transition metal surfaces has been extensively investigated by Beck and coworkers using the RAIRS technique.<sup>8-14</sup> By monitoring RAIRS of the methyl (CH<sub>3</sub>) adsorbate, which is one of the initial products of the methane dissociation, the initial sticking probability of methane can be measured accurately as a function of the incident energy and quantum state of the incident

methane, which provides valuable information on the state-specific<sup>8</sup> and coverage-dependent dissociation barrier. The technique can also be used to distinguish different isotopologues of an adsorbate as well as adsorption on different surface sites based on the small vibrational frequency shifts in the vibrational mode of the methyl adsorbate, offering insights into the site specificity and bond selectivity of the dissociation process. Apart from methane dissociative chemisorption, the methyl adsorbate is also an important intermediate in many industrial processes, so a detailed understanding of the RAIRS spectra of methyl species adsorbed on different sites on metal surfaces is highly desirable. Despite some theoretical calculations based on density functional theory (DFT), so the remain unexplained issues in the RAIRS spectra of CH<sub>3</sub> adsorbate on metal surfaces.

In particular, the methyl adsorbate has been detected by RAIRS on a number of Pt surfaces. As shown in Figure 1, the RAIRS spectrum upon CH<sub>4</sub> dissociation on Pt(111) (the red line) clearly shows a strong absorption peak at 2881 cm<sup>-1</sup>, <sup>9-10, 13</sup> which was assigned to the symmetric C-H stretching mode of adsorbed CH<sub>3</sub>. <sup>19-20</sup> Similar peaks assigned to terrace, step, and ridge sites have been observed for CH<sub>4</sub> dissociation on Pt(211)<sup>13</sup> and Pt(110)-(1 × 2) surfaces enabling site specific sticking coefficient measurements. <sup>14</sup> By examining the collision energy dependence of the sticking probability, these studies established unambiguously that the dissociation barrier at the step sites is significantly lower than that on terrace sites.

However, on Ni(111) the detection of a RAIRS signal due the symmetric C-H stretch of CH<sub>3</sub>(ads) following the dissociative chemisorption of methane surface has

been unsuccessful (see the blue line in Figure 1). This inability of RAIRS to detect CH<sub>3</sub> absorbed on Ni(111) was puzzling as CH<sub>3</sub> has been unambiguously detected using high-resolution electron energy loss spectroscopy (HREELS) by Ceyer and coworkers.<sup>21-23</sup> However, vibrational spectroscopy of adsorbates by HREELS follows different selection rules and can be used to detect both dipole active as well as dipole inactive adsorbate modes. The stark difference between the methyl RAIRS characteristics on Ni(111) and on Pt(111) begs the question about its origin.

In this Letter, we solve the puzzle of methyl RAIRS signal by computing the dipole moment of the system and analyzing its change with the specific vibrational mode. Being adsorbed at respectively preferred sites, we find on Pt(111) that the symmetric stretch mode of CH<sub>3</sub>\* causes a significant change in the normal component of dipole moment, thus resulting in strong IR activity, whereas the dipole moment change of the same mode becomes negligibly small on Ni(111), leading to essentially no IR activity. Decomposition of the dipole suggested the different behaviors are due largely to different charge transfer patterns between metal atoms and the adsorbate, rather than a simple surface electrostatic response to the molecular vibration. The charge transfer is in turn controlled by the adsorption site: methyl preferentially adsorbs on Pt(111) on a top site<sup>16-17, 24-25</sup> but on a hollow site on Ni(111).<sup>16, 26</sup> These insights help to establish the general propensity of IR activity for adsorbates on metal surfaces, advancing our understanding of adsorbate-metal interaction.

DFT calculations of adsorbed methyl on the Pt(111) and Ni(111) surfaces were performed with Vienna *Ab Initio* Simulation Package (VASP)<sup>27-28</sup> by using the Perdew-

Burke-Ernzerhof (PBE) functional<sup>29</sup>. Both surfaces were modeled by  $3 \times 3$  supercells with five slab layers in which the topmost two layers are allowed to relax. The  $5 \times 5 \times 1$  k-point meshes were used to sample the first Brillouin zone for all surface models. Dipole correction in the z direction was imposed to eliminate errors in total energy induced by artificial dipole-dipole interactions of the repeating slabs,<sup>30</sup> which concurrently yielded the z-component dipole moment ( $\mu_z$ ) of the system by the integration of the charge density distribution and position vector. Furthermore, charge transfer analysis was performed in terms of the density derived electrostatic and chemical (DDEC6) charge partitioning method implemented in the Chargemol program. More computational details are given in the Supporting Information (SI).

The static adsorption energies ( $E_{ad}$ ) and geometries of CH<sub>3</sub> on two metal surfaces along with their vibrational frequencies are shown in Table 1 and Figure S1 (in the SI). It is found that CH<sub>3</sub> prefers to adsorb on the top site of Pt(111) and the fcc site of Ni(111) with adsorption energies of -2.06 and -1.88 eV, respectively. This predicted site preference agrees well with the experimental assignments.<sup>23,33</sup> In both cases, the methyl adsorbate forms a pyramidal configuration and bonds with the metal surface with its carbon end. CH<sub>3</sub> binds less strongly to the top site of Ni(111) with  $E_{ad}$  of -1.57 eV and becomes unstable on the fcc site of Pt(111) with an approximate  $E_{ad}$  of  $\sim$ -1.33 eV (we can only find this geometry with a loose convergence criterion). The calculated adsorption energies and harmonic frequencies agree well with previous theoretical predictions, <sup>14, 16, 18, 26</sup> although the predicted frequencies are systematically higher than the experimental ones, <sup>14, 22, 33</sup> as discussed below, due presumably to the intrinsic error

in DFT as well as the harmonic approximation used in the theoretical calculations.

According to the surface IR selection rule, a specific vibration  $(Q_n)$  (with n being the label of this vibrational mode) is RAIRS active only if the corresponding dynamic dipole moment has a nonzero component perpendicular to the surface, namely  $\partial \mu_z / \partial Q_n \neq 0$  near the equilibrium geometry  $(Q_n = 0)$ . To reveal how this quantity correlates with the RAIRS intensity, we computed the variation of  $\mu_z$  as a function of  $Q_n$  for different vibrational modes and on different surface sites. Figure 2a illustrates the results for CH<sub>3</sub> adsorbed on the top site of Pt(111). It is clear that  $\mu_z$  varies monotonically with respect to  $Q_{ss}$  for symmetric C-H stretch ( $v_{ss}$ ). In contrast, it changes near-symmetrically with  $Q_{as1}$  and  $Q_{as2}$  for the two degenerate antisymmetric C-H stretch modes ( $v_{as1}$  and  $v_{as2}$ ) and reaches a minimum at  $Q_{as1} = 0$  and  $Q_{as2} = 0$ . We estimate that  $\partial \mu_z/\partial Q_{ss} = 0.22$  Debye/(Å·amu<sup>1/2</sup>) and  $\partial \mu_z/\partial Q_{as1} \approx \partial \mu_z/\partial Q_{as2} \approx 0$ at the equilibrium adsorption geometry, suggesting that  $v_{ss}$  is IR active but  $v_{as1}$  and  $v_{as2}$ are not. This prediction and the calculated harmonic frequency of the symmetric C-H stretching mode (2947 cm<sup>-1</sup>) are consistent with the measured RAIRS spectra shown in Figure 1 (red line), confirming the assignment of the strong speak around 2881 cm<sup>-1</sup> to  $v_{ss}$  of CH<sub>3</sub> on Pt(111). 9-10, 13 This can be understood from the group theory by which a vibrational mode that transforms to the same irreducible representation as  $\mu_z$ (translation z) is dipole-allowed. Specifically, the CH<sub>3</sub>-Pt(111) local structure on the top site can be approximated by the  $C_{3\nu}$ , 33 where  $\mu_z$  belongs to the totally symmetric  $A_1$  irreducible representation (irrep). Consequently,  $v_{ss}$  transforming as the  $A_1$  irrep will be IR active, while the doubly-degenerate antisymmetric C-H stretching modes

transforming as the E irrep will be IR inactive. These vibrational modes and their symmetry properties are visualized in Figure S2.

Next let us turn to discuss the absence of the IR signal for methyl on Ni(111). DFT calculations show that CH<sub>3</sub> binds preferably on the fcc site as opposed to the top site on Ni(111), with ~0.3 eV energy difference, consistent with the HREELS analysis of Ceyer et al. indicating that the CH<sub>3</sub> is adsorbed on the threefold hollow sites with C<sub>3v</sub> symmetry at 80 K.<sup>22-23</sup> Indeed, despite the difference in absolute values, we find in Figure 2b that similar behaviors of  $\mu_z$  of CH<sub>3</sub> on the top site of Ni(111) as these on Pt(111), e.g.,  $\mu_z$  change monotonically with  $Q_{ss}$ . This implies a similarly strong dynamic dipole moment for the v<sub>ss</sub> mode, which should be IR detectable if CH<sub>3</sub> stably binds at the top site. In the meantime, the asymmetric stretching modes remains inactive, as in the case of Pt(111). On the other hand, the variation of  $\mu_z$  with respect to the  $v_{ss}$ vibration of CH<sub>3</sub> on the fcc site reaches a minimum at  $Q_{ss} = 0$ , as shown in Figure 2c, which results in a tiny dynamic dipole moment with  $\partial \mu_z/\partial Q_{ss} \approx 0.02$ Debye/(Å·amu<sup>1/2</sup>) at the equilibrium adsorption geometry, similar to those for the asymmetric stretching modes. Since the IR intensity is proportional to the square of the dipole moment change, namely  $I_n \propto (\partial \mu_z/\partial Q_n)^2$ , the relative peak intensity of the CH<sub>3</sub> symmetric stretching mode on Ni(111) is estimated to be merely ~8‰ of that on Pt(111), making it very difficult to detect within the experimental noises. This result confirms the hypothesis proposed by Yang et al., 23 who assigned the HREELS peak at 2655 cm<sup>-1</sup> to the symmetric C-H stretch vibration of CH<sub>3</sub> adsorbed at the fcc site and suggested that this mode should be dipole active from symmetry analysis but may have

a very small dynamic dipole. In addition, our calculations reasonably predict a much lower frequency of  $v_{ss}$  (2783 cm<sup>-1</sup>) on Ni(111) than that on Pt(111) (2971 cm<sup>-1</sup>), giving rise to a difference by ~188 cm<sup>-1</sup>, on par with the observed ~226 cm<sup>-1</sup> for this "soft" C-H mode.<sup>22-23</sup> This mode softening was attributed to charge transfer from metals to antibonding orbitals of CH<sub>3</sub>, which is more pronounced at the fcc site on Ni(111) because the closer distance of the C-H bond to the metal surface than at the top site on Pt(111).<sup>16</sup> The comparison between Pt(111) and Ni(111) underscores the importance of electronic structure calculations in determining both the favorable adsorption site of molecule on surface and the dynamic dipole moment for a specific vibrational mode in interpreting the RAIRS spectra.

There are two limiting cases for a dipolar molecule interacting with a metal surface. In the first scenario, the molecular dipole has no contact with the surface and is only perturbed by the electrostatic response of the surface electrons when the dipole is close to the surface. This can typically be described by the dipole-image dipole interaction model, <sup>34</sup> in which the molecular dipole changes at different sites should be roughly the same. The other limit features chemisorption in which significant charge transfer between the adsorbate and metal surface takes place. As can be expected, this charge transfer is apparently site dependent, leading to different behaviors for the adsorbate dipole. To distinguish these two limiting cases, we decompose the total  $\mu_z$  in terms of contributions from the CH<sub>3</sub> adsorbate and from the metal-adsorbate interactions. As shown in Figure S3, the molecular dipole of the CH<sub>3</sub> moiety at the top and fcc sites behave rather differently along  $Q_{ss}$ , but both consistent with the change of the total

dipole moment of the system. This observation strongly argues against the simple electrostatic response model.

On the other hand, the associated charge transfer between CH<sub>3</sub> and the surface ( $\Delta q$ ) for the cases discussed in Figure 2 are shown as a function of  $Q_n$  in Figure 3. A positive  $\Delta q$  indicates charge transfer from the metal to the adsorbate and vice versa. At the top site of both the Ni(111) and Pt(111) surfaces (Figures 3a and 3b), the charge transfer is from the metal surface to the methyl adsorbate, which varies monotonously with  $Q_{ss}$ and gives rise to the same trend of the dipole moment change. By contrast, the charge transfer becomes negative on the fcc site of Ni(111) (Figure 3c), implying that the CH<sub>3</sub> adsorbate loses electrons to the metal surface. Moreover, the amount of charge transfer turns around at  $Q_{ss} = 0$  in this case, indicating that either elongating or shortening the C-H bond symmetrically leads to roughly the very similar variation in charge transfer from CH<sub>3</sub> to the Ni(111) surface. This trend is in general agreement with the corresponding dipole moment curve in Figure 2c. Similarly, the charge transfer variations for the antisymmetric stretch modes on Ni(111) and Pt(111) are all symmetric with respect to the equilibrium geometry, in line with the changes of dipole moments. These results suggest the dipole moment of the adsorbate on the metal surfaces is strongly correlated with the charge transfer, which is site-specific. This is a reasonable conclusion and is consistent with the chemisorption nature of this system. It is further supported by the large difference of the CH<sub>3</sub> symmetric stretching (harmonic) frequency at the top ( $\omega_{ss} = 2947 \text{ cm}^{-1}$ ) and fcc ( $\omega_{ss} = 2783 \text{ cm}^{-1}$ ) sites on Ni(111) as discussed above, which signals the significant change of the adsorption environment.

In conclusion, in this work we provide a first-principles explanation of the strong RAIRS signal of the symmetric C-H stretching vibration of methyl adsorbed on Pt(111) and its absence on Ni(111). Our calculations reveal that the RAIRS activity is dictated by the absorption site, which is in turn controlled by charge transfer, rather than electrostatic response of the surface electrons. At the top site of both metals, the methyl symmetric C-H stretching mode is IR active, but the activity is quenched at fcc site. On Pt(111), methyl preferentially adsorbs at the top site, resulting in the experimentally observable RAIRS activity. On Ni(111), however, it prefers the adsorption at the fcc site, leading to undetectable RAIRS activity, although the mode can still be detected using other techniques such as HREELS. These new insights help to gain a deeper understanding of site specificity of adsorbate optical activity, which is vital to extract valuable information on surface reactions. This computational scheme also offers an efficient way to predict IR activity of adsorbates on metal surfaces in future reactivity studies using RAIRS as a detection method.

Acknowledgements: This work is supported by National Natural Science Foundation of China (22073089 and 22033007 to B.J.), K. C. Wong Education (GJTD-2020-15 to B.J.), the Fundamental Research Funds for Central Universities (WK2060000017 to B.J.), by the Swiss National Science Foundation (Grant No. 200020\_159689 to R.D.B.), and by National Science Foundation (Grant. No. CHE-1951328 to H.G.). We thank Li Yang, XiJun Wang, and Prof. Jun Jiang for helpful discussion on the dipole calculations. RDB would like to thank Dr Li Chen and Dr. Helen Chadwick for their contributions

to the RAIRS spectrometer at EPFL. H.G. also thanks the Alexander von Humboldt Foundation for a Humboldt Research Award. Numerical calculations have been done on the Hefei advanced computing center and the supercomputing center of USTC.

## References

- 1. Hoffmann, F., Infrared Reflection-Absorption Spectroscopy of Adsorbed Molecules. *Surf. Sci. Rep.* **1983**, *3*, 107-192.
- 2. Trenary, M., Reflection Absorption Infrared Spectroscopy and the Structure of Molecular Adsorbates on Metal Surfaces. *Annu. Rev. Phys. Chem.* **2000**, *51*, 381-403.
- 3. Mukerji, R. J.; Bolina, A. S.; Brown, W. A., A Rairs and Tpd Investigation of the Adsorption of Co on Pt(211). *Surf. Sci.* **2003**, *527*, 198-208.
- 4. Walsh, A. J.; van Lent, R.; Auras, S. V.; Gleeson, M. A.; Berg, O. T.; Juurlink, L. B. F., Step-Type and Step-Density Influences on Co Adsorption Probed by Reflection Absorption Infrared Spectroscopy Using a Curved Pt(1 1 1) Surface. *J. Vac. Sci. Technol. A* **2017**, *35*, 03E102.
- 5. Raval, R., Probing the Nature of Molecular Chemisorption Using Rairs. *Surf Sci.* **1995**, *331*, 1-10.
- 6. Chadwick, H.; Beck, R. D., Quantum State Resolved Gas-Surface Reaction Dynamics Experiments: A Tutorial Review. *Chem. Soc. Rev.* **2016**, *45*, 3576-3594.
- 7. Chadwick, H.; Beck, R. D., Quantum State—Resolved Studies of Chemisorption Reactions. *Annu. Rev. Phys. Chem.* **2017**, *68*, 39-61.
- 8. Gutiérrez-González, A.; Beck, R. D., Quantum State and Surface-Site-Resolved Studies of Methane Chemisorption by Vibrational Spectroscopies. *Phys. Chem. Chem. Phys.* **2020**, *22*, 17448-17459.
- 9. Ueta, H.; Chen, L.; Beck, R. D.; Colon-Diaz, I.; Jackson, B., Quantum State-Resolved Ch<sub>4</sub> Dissociation on Pt(111): Coverage Dependent Barrier Heights from Experiment and Density Functional Theory. *Phys. Chem. Chem. Phys.* **2013**, *15*, 20526-20535.
- 10. Chen, L.; Ueta, H.; Bisson, R.; Beck, R. D., Vibrationally Bond-Selected Chemisorption of Methane Isotopologues on Pt(111) Studied by Reflection Absorption Infrared Spectroscopy. *Faraday Discuss.* **2012**, *157*, 285-295.
- 11. Hundt, P. M.; Ueta, H.; van Reijzen, M. E.; Jiang, B.; Guo, H.; Beck, R. D., Bond-Selective and Mode-Specific Dissociation of Ch₃d and Ch₂d₂ on Pt(111). *J. Phys. Chem. A* **2015**, *119*, 12442-12448.
- 12. Gutiérrez-González, A.; Crim, F. F.; Beck, R. D., Bond Selective Dissociation of Methane (Ch₃d) on the Steps and Terraces of Pt(211). *J. Chem. Phys.* **2018**, *149*, 074701.
- 13. Chadwick, H.; Guo, H.; Gutiérrez-González, A.; Menzel, J. P.; Jackson, B.; Beck, R. D., Methane Dissociation on the Steps and Terraces of Pt(211) Resolved by Quantum State and Impact Site. *J. Chem. Phys.* **2018**, *148*, 014701.
- 14. Gutiérrez-González, A.; Torio, M. E.; Busnengo, H. F.; Beck, R. D., Site Selective Detection of Methane Dissociation on Stepped Pt Surfaces. *Top. Catal.* **2019**, *62*, 859-873.
- 15. Chorkendorff, I.; Niemantsverdriet, J. W., *Concepts of Modern Catalysis and Kinetics*, Wiley-VCH: Weinheim, 2003.
- 16. Michaelides, A.; Hu, P., Softened C–H Modes of Adsorbed Methyl and Their Implications for Dehydrogenation: An Ab Initio Study. *J. Chem. Phys.* **2001**, *114*, 2523-2526.
- 17. Ford, D. C.; Xu, Y.; Mavrikakis, M., Atomic and Molecular Adsorption on Pt(111). *Surf. Sci.* **2005**, *587*, 159-174.
- 18. Torio, M. E.; Busnengo, H. F., Site-Specific Product Selectivity of Stepped Pt Surfaces for Methane Dehydrogenation. *J. Phys. Chem. C* **2020**, *124*, 19649-19654.
- 19. Oakes, D. J.; McCoustra, M. R. S.; Chesters, M. A., Dissociative Adsorption of Methane on

- Pt(111) Induced by Hyperthermal Collisions. Faraday Disc. 1993, 96, 325-336.
- 20. Fairbrother, D. H.; Peng, X. D.; Trenary, M.; Stair, P. C., Surface Chemistry of Methyl Groups Adsorbed on Pt(111). *J. Chem. Soc. Faraday Trans.* **1995**, *91*, 3619-3625.
- 21. Johnson, A. D.; Daley, S. P.; Utz, A. L.; Ceyer, S. T., The Chemistry of Bulk Hydrogen: Reaction of Hydrogen Embedded in Nickel with Adsorbed Ch3. *Science* **1992**, *257*, 223–225.
- 22. Ceyer, S. T., Translational and Collision-Induced Activation of Methane on Nickel(111): Phenomena Connecting Ultra-High-Vacuum (Uhv) Surface Science to High-Pressure Heterogeneous Catalysis. *Langmuir* **1990**, *6*, 82-87.
- 23. Yang, Q. Y.; Maynard, K. J.; Johnson, A. D.; Ceyer, S. T., The Structure and Chemistry of Ch3 and Ch Radicals Adsorbed on Ni(111). *J. Chem. Phys.* **1995**, *102*, 7734-7749.
- 24. Chen, Y.; Vlachos, D. G., Hydrogenation of Ethylene and Dehydrogenation and Hydrogenolysis of Ethane on Pt(111) and Pt(211): A Density Functional Theory Study. *J. Phys. Chem. C* **2010**, *114*, 4973-4982.
- 25. Vines, F.; Lykhach, Y.; Staudt, T.; Lorenz, M. P.; Papp, C.; Steinruck, H. P.; Libuda, J.; Neyman, K. M.; Gorling, A., Methane Activation by Platinum: Critical Role of Edge and Corner Sites of Metal Nanoparticles. *Chemistry* **2010**, *16*, 6530-6539.
- 26. Nave, S.; Jackson, B., Methane Dissociation on Ni(111) and Pt(111): Energetic and Dynamical Studies. *J. Chem. Phys.* **2009**, *130*, 054701.
- 27. Kresse, G.; Furthmuller, J., Efficient Iterative Schemes for Ab Initio Total-Energy Calculations Using Plane Wave Basis Set. *Phys. Rev. B* **1996**, *54*, 11169-11186.
- 28. Kresse, G.; Furthmuller, J., Efficiency of Ab Initio Total Energy Calculations for Metals and Semiconductors Using Plane Wave Basis Set. *Comp. Mater. Sci.* **1996**, *6*, 15-50.
- 29. Perdew, J. P.; Burke, K.; Ernzerhof, M., Generalized Gradient Approximation Made Simple. *Phys. Rev. Lett.* **1996**, *77*, 3865-3868.
- 30. Neugebauer, J.; Scheffler, M., Adsorbate-Substrate and Adsorbate-Adsorbate Interactions of Na and K Adlayers on Al(111). *Phys. Rev. B* **1992**, *46*, 16067-16080.
- 31. Manz, T. A.; Limas, N. G., Introducing Ddec6 Atomic Population Analysis: Part 1. Charge Partitioning Theory and Methodology. *RSC Advances* **2016**, *6*, 47771-47801.
- 32. Limas, N. G.; Manz, T. A., Introducing Ddec6 Atomic Population Analysis: Part 2. Computed Results for a Wide Range of Periodic and Nonperiodic Materials. *RSC Advances* **2016**, *6*, 45727-45747.
- 33. Radhakrishnan, G.; Stenzel, W.; Hemmen, R.; Conrad, H.; Bradshaw, A. M., The Photon-Induced Reactions of Chemisorbed Ch3br on Pt{111}. *J. Chem. Phys.* **1991**, *95*, 3930-3938.
- 34. Lennard-Jones, J. E., Processes of Adsorption and Diffusion on Solid Surfaces. *Trans. Faraday Society* **1932**, *28*, 333.

Table 1. Calculated adsorption energies ( $E_{ad}$ , in eV) and harmonic vibrational frequencies (in cm<sup>-1</sup>) of CH<sub>3</sub> at different surface sites on Pt(111) and Ni(111) using the PBE functional.  $\nu_{as1(2)}$  and  $\nu_{ss}$  represent the first(second) asymmetric and symmetric C-H stretch modes, respectively. Experimental assigned peaks for C-H stretch modes from RAIRS and HREELS spectra are shown for comparison.

property -	Pt(111)		Ni(111)		Expt. Freq.	
	top	fcc	top	fcc	Pt(111)	Ni(111)
$E_{\rm ad}$	-2.06	-1.33	-1.57	-1.88	-	-
$v_{as1}$	3080	2921	3042	2850	-	2730 <sup>a</sup>
$V_{as2}$	3079	2915	3042	2846		
$\mathcal{V}_{SS}$	2971	2839	2947	2783	2839 <sup>b</sup> , 2881 <sup>c</sup>	2655a

<sup>&</sup>lt;sup>a</sup>from Ref. 22

<sup>&</sup>lt;sup>b</sup>from Ref. 33

<sup>&</sup>lt;sup>c</sup>from Ref. 14

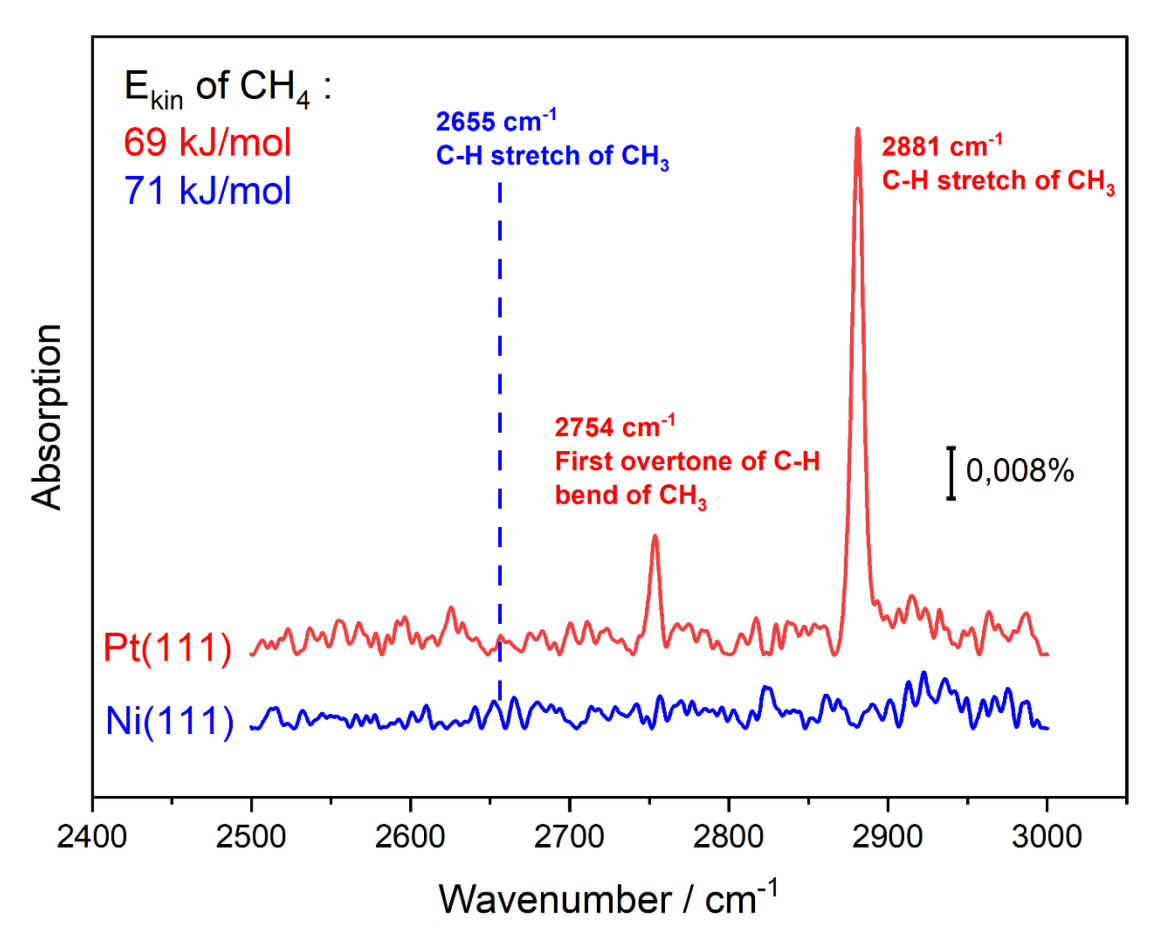


Figure 1. RAIRS spectra taken following exposure of a 3% CH<sub>4</sub> in He molecular beam with incident kinetic energies of 69 and 71 kJ/mol on Pt(111) (red line) and Ni(111) (blue line) at surface temperatures of 150 and 120 K, respectively. On Pt(111), the symmetric C-H stretch mode of CH<sub>3</sub> was detected at 2881 cm<sup>-1</sup> and the first overtone of the C-H bending mode is at 2754 cm<sup>-1</sup>. On Ni(111), no RAIRS signal was detected above the background noise. The blue dash line labels the peak position of the symmetric C-H stretch mode at 2655 cm<sup>-1</sup> observed by HREELS spectroscopy.<sup>23</sup>

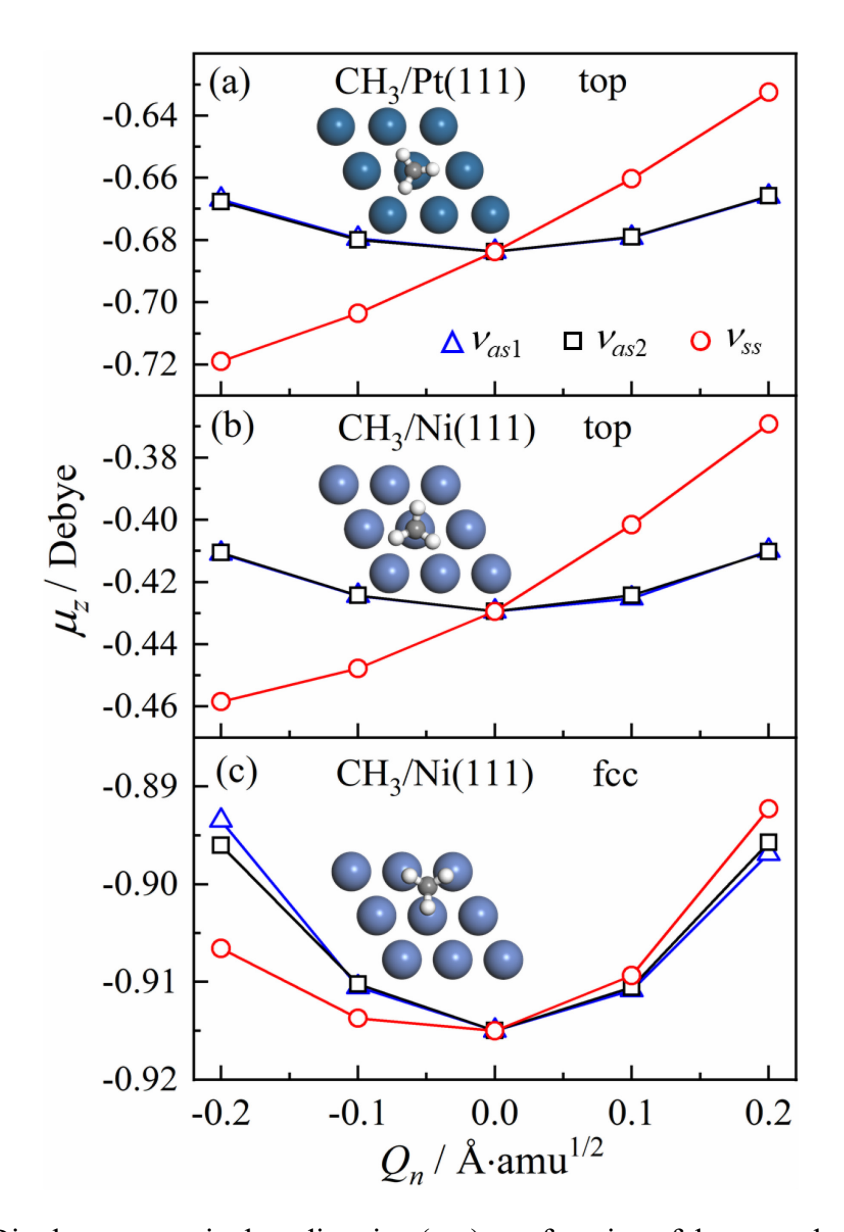


Figure 2. Dipole moments in the z direction ( $\mu_z$ ) as a function of the normal coordinates ( $Q_n$ ) of the antisymmetric ( $v_{as1}$  and  $v_{as2}$ ) and symmetric ( $v_{ss}$ ) C-H stretching modes of CH<sub>3</sub> adsorbed at the top sites of (a) Pt(111) and (b) Ni(111), (c) the fcc site of Ni(111).

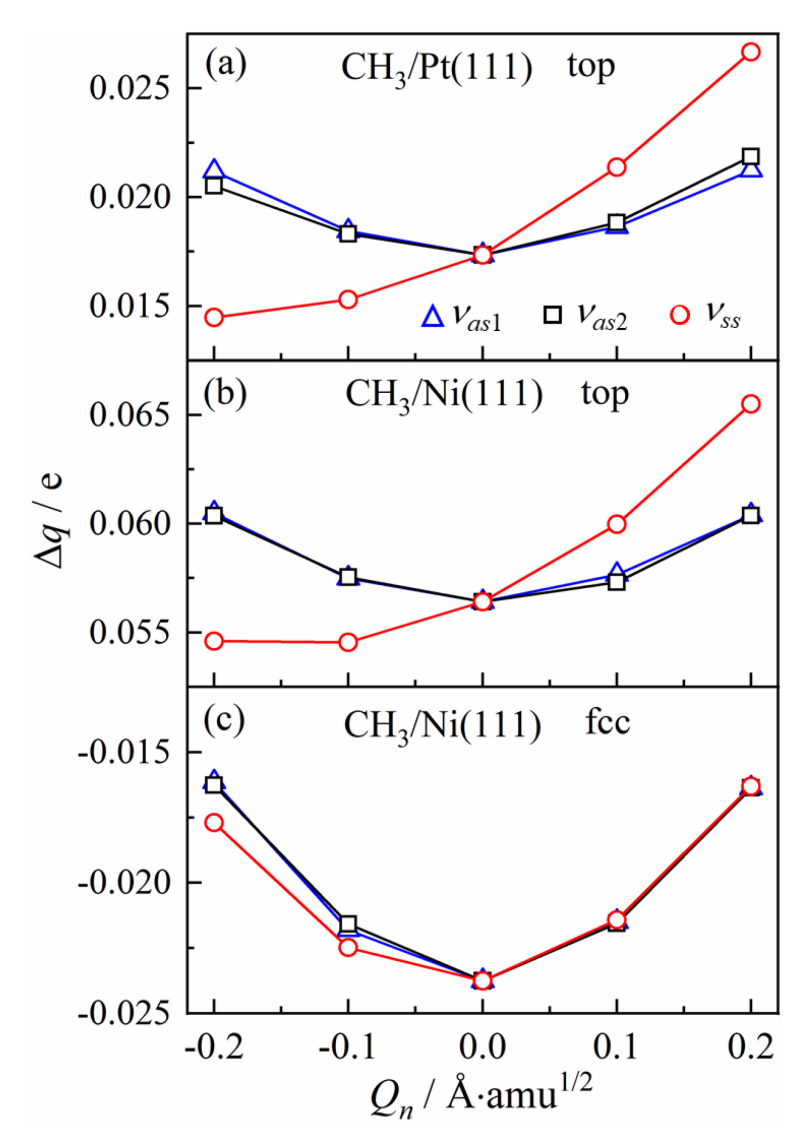


Figure 3. Charge transfer from the surface to CH<sub>3</sub> as a function of  $Q_n$  of the  $v_{as1}$ ,  $v_{as2}$  and  $v_{ss}$  modes for (a) CH<sub>3</sub>/Pt(111) and (b) CH<sub>3</sub>/Ni(111) at the top site and (c) CH<sub>3</sub>/Ni(111) at the fcc site.